THE ASTROPHYSICAL JOURNAL, 686:694–700, 2008 October 10

TRANSVERSE OSCILLATIONS OF LONGITUDINALLY STRATIFIED CORONAL LOOPS WITH VARIABLE CROSS SECTION

M. S. RUDERMAN, G. VERTH, AND R. ERDÉLYI
Solar Physics and Space Plasma Research Centre (SP[2]RC), University of Sheffield, Hicks Building, Hounsfield Road, Sheffield, S3 7RH, England, UK; M.S.Ruderman@sheffield.ac.uk
Received 2008 June 3; accepted 2008 June 26

ABSTRACT

We consider transverse oscillations of coronal loops that have both variable circular cross-sectional area and plasma density in the longitudinal direction. The primary focus of this paper is to study the eigenmodes of these oscillations. Implementing the method of asymptotic expansions with the ratio of the loop radius to length as a small parameter, a second-order ordinary differential equation is derived describing the displacement of the loop axis. Together with the boundary conditions at the tube ends that follow from the frozen-in condition, this equation constitutes the Sturm-Liouville problem determining the eigenfrequencies and eigenmodes. Our results are relevant to the magnetoseismological method of estimating the coronal density scale height by using the observed ratio of the fundamental frequency and first overtone of loop kink oscillations. It is shown that this method is very sensitive to the tube expansion factor, which is the ratio of the tube radii at the apex and footpoints. The estimated scale height is a monotonically decreasing function of the expansion factor.

Subject headings: MHD — Sun: corona — Sun: magnetic fields — Sun: oscillations

1. INTRODUCTION

Transverse oscillations of coronal magnetic loops are one of the most spectacular manifestations of the wave motion in the solar atmosphere. These oscillations were observed by the *TRACE* spacecraft and first reported by Aschwanden et al. (1999) and Nakariakov et al. (1999). Nakariakov et al. (1999) interpreted these oscillations as fast kink modes of magnetic flux tubes. For a recent review on MHD waves and oscillations in the solar atmosphere see, e.g., Banerjee et al. (2007). The transverse oscillations of coronal loops are especially interesting for theorists and coronal seismologists, since they provide an ideal diagnostic signature of the fine structure of the corona. In a pioneering work by Nakariakov & Ofman (2001), they were used to estimate the magnitude of magnetic field in coronal loops.

In the initial theoretical works, the simplest model of coronal loops was used. This model was a straight homogeneous magnetic tube with fixed ends. Later, more realistic and complex models were developed. In particular, Andries et al. (2005b) and Goossens et al. (2006) numerically studied the effect of the longitudinal density stratification on the transverse oscillations of coronal loops. Dymova & Ruderman (2005, 2006a) showed that, in the thin-tube approximation, frequencies and eigenfunctions of the fast kink mode in a magnetic tube with longitudinally stratified plasma density are determined by the classical Sturm-Liouville problem.

Recently, Verth & Erdélyi (2008) generalized the results obtained by Dymova & Ruderman by also allowing the cross-sectional area of the flux tube to vary in the longitudinal direction. In their derivation they assumed that the expansion factor, which is the ratio of the tube radii at the apex point and at the footpoint, is small. The aim of this paper is to derive the equation determining the eigenvalues and eigenfrequencies of longitudinally stratified magnetic tubes with variable cross sections that is valid for arbitrary expansion factors. The paper is organized as follows. In § 2 we discuss general properties of an equilibrium configuration with expanding magnetic tubes. In § 3 the linearized ideal MHD equations will be transformed to magnetic flux coordinates. In § 4 the equation describing the eigenfrequencies and eigenfunctions of loop kink oscillations is derived. In § 5 the implication of our results for coronal seismology is discussed. Section 6 contains the summary of the results obtained and our conclusions.

2. EQUILIBRIUM CONFIGURATION

We consider an equilibrium configuration in the form of a straight magnetic tube with variable cross section and the density varying along the tube (see Fig. 1). In what follows we use cylindrical coordinates r, φ, and z with the z-axis coinciding with the tube axis. The tube ends are frozen in a dense photospheric plasma at $z = \pm L$. The tube radius R varies along the tube, $R = R(z)$. The plasma density ρ has a jump at the tube boundary and depends on z, so that $\rho = \rho_i(z)$ for $r < R(z)$ and $\rho = \rho_e(z)$ for $r > R(z)$.

The tube is assumed to be thin, $R/L = O(\epsilon)$, where $\epsilon \ll 1$. The equilibrium magnetic field has two components, r and z, and is independent of φ, so that $\boldsymbol{B} = \boldsymbol{B}(r, z)$. It follows from the solenoidal condition that $\boldsymbol{B}$ can be expressed in terms of the flux function ψ,

$$B_r = -\frac{1}{r}\frac{\partial\psi}{\partial z}, \quad B_z = \frac{1}{r}\frac{\partial\psi}{\partial r}. \tag{1}$$

The electrical current, $\boldsymbol{J} = \nabla \times \boldsymbol{B}/\mu_0$, where μ_0 is the magnetic permeability of free space, is in the φ-direction, $\boldsymbol{J} = J\boldsymbol{e}_\varphi$, where $\boldsymbol{e}_\varphi$ is the unit vector in the φ-direction. Then, the r-component of the Lorentz force, $\boldsymbol{J} \times \boldsymbol{B}$, is equal to JB_z. We assume that $B_z \neq 0$ everywhere and use the cold plasma approximation. Then it follows from the equilibrium equation, $\boldsymbol{J} \times \boldsymbol{B} = 0$, that $J = 0$, i.e., the magnetic field is potential. This implies that ψ satisfies the equation

$$r\frac{\partial}{\partial r}\left(\frac{1}{r}\frac{\partial\psi}{\partial r}\right) + \frac{\partial^2\psi}{\partial z^2} = 0. \tag{2}$$

The equation of the tube boundary is $\psi(r, z) = \psi_0$, where ψ_0 is constant. In what follows we assume that $\boldsymbol{B} \to B_\infty \boldsymbol{e}_z$ as $r \to \infty$, where $B_\infty > 0$ is a constant and $\boldsymbol{e}_z$ is the unit vector in the z-direction.

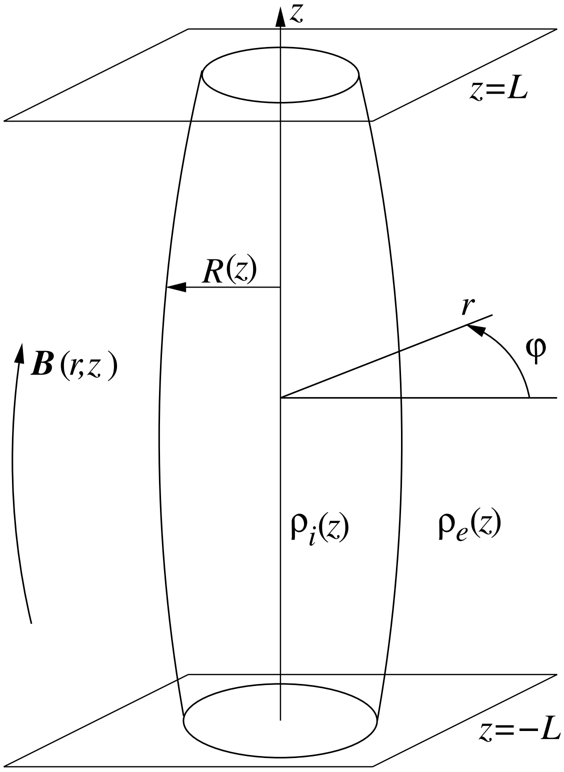

FIG. 1.—Sketch of the equilibrium configuration.

We obtain an example of the potential magnetic field satisfying this condition if we take

$$\psi = (1/2)B_\infty r^2 + \psi_* r J_1(r/l)\cosh(z/l), \tag{3}$$

where ψ_* and l are arbitrary constants and $J_1(x)$ is the Bessel function of the first kind and first order. The parameter l can be considered as the characteristic scale of variation of the magnetic equilibrium field. Then,

$$B_r = -\frac{\psi_*}{l} J_1\left(\frac{r}{l}\right)\sinh\left(\frac{z}{l}\right),$$
$$B_z = B_\infty + \frac{\psi_*}{l} J_0\left(\frac{r}{l}\right)\cosh\left(\frac{z}{l}\right), \tag{4}$$

where J_0 is the Bessel function of the first kind and zeroth order. Let j_1 be the first positive root of $J_1(x)$ so that $J_1(j_1) = 0$. Then, since $J_0'(x) = -J_1(x)$, where the prime indicates the derivative, $J_0(x)$ takes its minimum value at $x = j_1$, and $J_0(x)$ takes its maximum value of 1 at $x = 0$. Now, taking

$$-lB_\infty < \psi_*\cosh(L/l) < lB_\infty/|J_0(j_1)| \approx 2.5lB_\infty, \tag{5}$$

we obtain $B_z > 0$ everywhere. Equation (4) takes an especially simple form if we take $l \gtrsim L$ and restrict the attention to the tube interior and its vicinity assuming $r \ll L$. Then, using the approximate expressions for the Bessel functions valid for small values of the argument (see, e.g., Abramowitz & Stegun 1964),

$$J_0(x) \approx 1, \quad J_1(x) \approx \frac{x}{2}, \tag{6}$$

we obtain

$$B_r \approx -\frac{\psi_* r}{2l^2}\sinh\left(\frac{z}{l}\right), \quad B_z \approx B_\infty + \frac{\psi_*}{l}\cosh\left(\frac{z}{l}\right). \tag{7}$$

The approximate equation of the tube boundary is

$$R(z) \approx l\sqrt{\frac{2\psi_0}{l^2 B_\infty + l\psi_*\cosh(z/l)}}, \tag{8}$$

where ψ_0 is a positive constant. Note that the tube expands $[R(0) > R(\pm L)]$ when $\psi_* > 0$, while it contracts $[R(0) < R(\pm L)]$ when $\psi_* < 0$. In what follows we assume that $\psi_* > 0$, i.e., the tube expands. The condition that the tube is thin, $R(z) \ll L$, takes the form

$$\psi_0 \ll L^2(B_\infty + \psi_*/l). \tag{9}$$

The tube radius at the footpoints, $R_f = R(\pm L)$, is given by

$$R_f \approx l\sqrt{\frac{2\psi_0}{l^2 B_\infty + l\psi_*\cosh(L/l)}}. \tag{10}$$

The tube expansion factor, $\lambda = R(0)/R_f$, is given by

$$\lambda \approx \sqrt{\frac{lB_\infty + \psi_*\cosh(L/l)}{lB_\infty + \psi_*}}. \tag{11}$$

After some algebra, the condition that $B_z > 0$ given by equation (5) can be rewritten in the approximate form

$$\lambda^2 < \lambda_m^2 \approx \frac{[1 - J_0(j_1)]\cosh(L/l)}{1 - J_0(j_1)\cosh(L/l)} \tag{12}$$
$$\approx \frac{1.4\cosh(L/l)}{1 + 0.4\cosh(L/l)}. \tag{13}$$

We see that λ_m is a monotonically increasing function of L/l, $\lambda_m \to 1$ when $L/l \to 0$, and $\lambda_m \to [1 - 1/J_0(j_1)]^{1/2} \approx 1.87$ as $L/l \to \infty$. Using equations (10) and (11) we can rewrite equation (8) for $R(z)$ as

$$R(z) = R_f\lambda\sqrt{\frac{\cosh(L/l) - 1}{\cosh(L/l) - \lambda^2 + (\lambda^2 - 1)\cosh(z/l)}}. \tag{14}$$

We have to emphasize the important property of this particular model: it can describe only magnetic tubes with relatively small expansion factors, definitely smaller than 1.87. Note, however, that this restriction is related to a particular background state that we only consider as an example. The derivation of the governing equation is free from any restrictions of this type except that $R(z) \ll L$ for any z.

In what follows we consider an arbitrary magnetic field given by equations (1) and (2). However, we impose the restriction that $B_z > 0$ everywhere and that the characteristic scale of the magnetic field variation is L. Since the tube is thin, $R(z)/L = O(\epsilon)$, $\epsilon \ll 1$, the second condition implies that, in the vicinity of the magnetic tube, we can approximate ψ by the first term of its expansion in the Taylor series. Since the tube axis is a magnetic field line, $\psi = \text{const}$ at $r = 0$. Then, it follows that the approximate expression for ψ is

$$\psi = \frac{1}{2} r^2 h(z). \tag{15}$$

Using equation (1) we obtain the approximate expressions for the magnetic field components,

$$B_r = -\frac{r}{2}h'(z), \quad B_z = h(z). \tag{16}$$

Recall that equations (15) and (16) are only valid in the vicinity of the magnetic tube, where $r/L = O(\epsilon)$. Using equation (16), we obtain

$$B = \sqrt{B_r^2 + B_z^2} = B_z + O(\epsilon^2) = h(z) + O(\epsilon^2). \tag{17}$$

It also follows from the magnetic flux conservation that

$$h(z)R^2(z) = \text{const}. \tag{18}$$

3. TRANSFORMATION OF LINEAR MHD EQUATIONS TO FLUX COORDINATES

To describe the plasma motion we use the linear ideal MHD equations for a cold plasma,

$$\frac{\partial^2 \boldsymbol{\xi}}{\partial t^2} = \frac{1}{\mu_0 \rho}(\nabla \times \boldsymbol{b}) \times \boldsymbol{B}, \tag{19}$$

$$\boldsymbol{b} = \nabla \times (\boldsymbol{\xi} \times \boldsymbol{B}), \tag{20}$$

where $\boldsymbol{\xi} = (\xi_r, \xi_\varphi, \xi_z)$ is the plasma displacement and $\boldsymbol{b} = (b_r, b_\varphi, b_z)$ is the magnetic field perturbation.

Introducing the parallel and perpendicular components of $\boldsymbol{\xi}$ and $\boldsymbol{b}$,

$$\xi_\parallel = \boldsymbol{\xi} \cdot \boldsymbol{B}/B, \quad \xi_\perp = (B_z \xi_r - B_r \xi_z)/B, \tag{21}$$

$$b_\parallel = \boldsymbol{b} \cdot \boldsymbol{B}/B, \quad b_\perp = (B_z b_r - B_r b_z)/B, \tag{22}$$

and the magnetic pressure perturbation

$$P = \frac{1}{\mu_0} B b_\parallel = \frac{1}{\mu_0}\boldsymbol{b} \cdot \boldsymbol{B}, \tag{23}$$

we rewrite equations (19) and (20) in components as

$$\begin{aligned}\frac{\mu_0 \rho}{B}\frac{\partial^2 \xi_\perp}{\partial t^2} = \mu_0 B_r \frac{\partial}{\partial z}\left(\frac{P}{B^2}\right) - \mu_0 B_z \frac{\partial}{\partial r}\left(\frac{P}{B^2}\right) \\ + rB_r \frac{\partial}{\partial r}\left(\frac{b_\perp}{rB}\right) + B_z \frac{\partial}{\partial z}\left(\frac{b_\perp}{B}\right),\end{aligned} \tag{24}$$

$$\mu_0 \rho \frac{\partial^2 \xi_\varphi}{\partial t^2} = \frac{B_r}{r}\frac{\partial (r b_\varphi)}{\partial r} + B_z \frac{\partial b_\varphi}{\partial z} - \frac{\mu_0}{r}\frac{\partial P}{\partial \varphi}, \tag{25}$$

$$B b_\perp = B_z \frac{\partial (B\xi_\perp)}{\partial z} + \frac{B_r}{r}\frac{\partial (rB\xi_\perp)}{\partial r}, \tag{26}$$

$$b_\varphi = \frac{\partial (B_r \xi_\varphi)}{\partial r} + \frac{\partial (B_z \xi_\varphi)}{\partial z}, \tag{27}$$

$$\mu_0 P = B_r \frac{\partial (B\xi_\perp)}{\partial z} - \frac{B_z}{r}\frac{\partial (rB\xi_\perp)}{\partial r} - \frac{B^2}{r}\frac{\partial \xi_\varphi}{\partial \varphi}. \tag{28}$$

Note that $\xi_\parallel = 0$.

Now we use ψ as an independent variable instead of r, so that $r = r(\psi, z)$. For an arbitrary function f we have the following relations,

$$\frac{\partial f}{\partial r} = rB_z \frac{\partial f}{\partial \psi}, \quad \frac{\partial f}{\partial z} = \frac{\partial f}{\partial z} - rB_r \frac{\partial f}{\partial \psi}. \tag{29}$$

When deriving these relations we have used equation (1). Differentiating the identity $\psi = \psi(r(\psi, z), z)$ with respect to z and using equation (1), we obtain

$$\frac{\partial r}{\partial z} = \frac{B_r}{B_z}. \tag{30}$$

Differentiating the identity $r = r(\psi(r, z), z)$ with respect to z and using equations (1) and (30) yields

$$\frac{\partial r}{\partial \psi} = \frac{1}{rB_z}. \tag{31}$$

Using equations (29)–(31) and the equation $\nabla \cdot \boldsymbol{B} = 0$, we transform equations (24)–(28) to

$$\frac{\partial^2 u}{\partial t^2} = \frac{B^2 B_r}{\rho}\frac{\partial Q}{\partial z} - \frac{rB^4}{\rho}\frac{\partial Q}{\partial \psi} + \frac{rB^2 B_z}{\mu_0 \rho}\frac{\partial}{\partial r}\left(\frac{b_\perp}{rB}\right), \tag{32}$$

$$\frac{\partial^2 \xi_\varphi}{\partial t^2} = \frac{B_z}{\mu_0 r \rho}\frac{\partial (r b_\varphi)}{\partial z} - \frac{B^2}{r\rho}\frac{\partial Q}{\partial \varphi}, \tag{33}$$

$$b_\perp = \frac{B_z}{rB}\frac{\partial (ru)}{\partial z}, \tag{34}$$

$$b_\varphi = rB_z \frac{\partial}{\partial z}\left(\frac{\xi_\varphi}{r}\right), \tag{35}$$

$$Q = \frac{B_r}{\mu_0 B^2}\frac{\partial u}{\partial z} - \frac{r}{\mu_0}\frac{\partial u}{\partial \psi} - \frac{B_z u}{\mu_0 r B^2} - \frac{1}{\mu_0 r}\frac{\partial \xi_\varphi}{\partial \varphi}, \tag{36}$$

where

$$u = B\xi_\perp, \quad Q = \frac{P}{B^2}. \tag{37}$$

Eliminating $b_\perp$ and b_φ from equations (32)–(35), we obtain the system of two equations for u, ξ_φ, and Q,

$$\begin{aligned}\frac{\partial^2 u}{\partial t^2} = \frac{rB^2 B_z}{\mu_0 \rho}\frac{\partial}{\partial z}\left[\frac{B_z}{r^2 B^2}\frac{\partial (ru)}{\partial z}\right] \\ + \frac{B^2}{\rho}\left(B_r \frac{\partial Q}{\partial z} - rB^2 \frac{\partial Q}{\partial \psi}\right),\end{aligned} \tag{38}$$

$$\frac{\partial^2 \xi_\varphi}{\partial t^2} = \frac{B_z}{\mu_0 r \rho}\frac{\partial}{\partial z}\left[r^2 B_z \frac{\partial}{\partial z}\left(\frac{\xi_\varphi}{r}\right)\right] - \frac{B^2}{r\rho}\frac{\partial Q}{\partial \varphi}. \tag{39}$$

These equations together with equation (36) constitute the closed system of equations for the variables u, ξ_φ, and Q. It is valid for any equilibrium magnetic field determined by equations (1) and (2). If we now take ψ and $\boldsymbol{B}$ given by equations (15) and (16), then this system of equations is substantially simplified. In that case,

$$r = \sqrt{\frac{2\psi}{h(z)}}. \tag{40}$$

Then, using equations (16), (17), and (40), we reduce equations (36), (38), and (39) to

$$\frac{\partial^2 u}{\partial t^2} = \frac{h\sqrt{h}}{\rho}\left[\frac{h}{\mu_0}\frac{\partial^2}{\partial z^2}\left(\frac{u}{\sqrt{h}}\right) - \sqrt{2\psi}\left(\frac{h'}{2}\frac{\partial Q}{\partial z} + h^2 \frac{\partial Q}{\partial \psi}\right)\right], \tag{41}$$

$$\frac{\partial^2 \xi_\varphi}{\partial t^2} = \frac{h\sqrt{h}}{\rho}\left[\frac{1}{\mu_0}\frac{\partial^2(\xi_\varphi\sqrt{h})}{\partial z^2} - \frac{h}{\sqrt{2\psi}}\frac{\partial Q}{\partial \varphi}\right], \tag{42}$$

$$Q = \frac{-1}{\mu_0\sqrt{2h\psi}}\left(\frac{h'\psi}{h^2}\frac{\partial u}{\partial z} + 2\psi\frac{\partial u}{\partial \psi} + u + h\frac{\partial \xi_\varphi}{\partial \varphi}\right). \tag{43}$$

This system of equations will be used in § 4 to derive the equation determining the eigenmodes and eigenfrequencies of the kink oscillations of the magnetic tube. Since equations (15) and (16) are only valid in the vicinity of the magnetic tube, equations (41)–(43) are also only valid in this vicinity.

4. STURM-LIOUVILLE PROBLEM FOR KINK OSCILLATIONS

As already stated above, we assume that the tube is thin. This implies that the characteristic scale of the variation of perturbations in the longitudinal direction is much larger than that in the radial direction. This observation inspires us to introduce the stretching variable in the longitudinal direction, $\zeta = \epsilon z$. In what follows we consider only kink oscillations and look for eigenmodes. Therefore, we take perturbations of all variables proportional to $\exp(-i\omega t + i\varphi)$. Let us introduce the characteristic Alfvén speed inside the tube, $V_A = B_0/(\mu_0\rho_0)^{1/2}$, where B_0 and ρ_0 are the typical values of the magnetic field and density inside the tube, respectively. Then, the typical frequency of kink oscillations is $\pi V_A/L$, which is much smaller than the reciprocal of the Alfvén time calculated using the tube radius, $\tau_A^{-1} = V_A/R(0)$. This implies that one needs to introduce the scaled frequency $\Omega = \epsilon^{-1}\omega$.

Now equations (41)–(43) are rewritten as

$$-\epsilon^2\Omega^2 u = \frac{h\sqrt{h}}{\rho}\left[\epsilon^2\frac{h}{\mu_0}\frac{\partial^2}{\partial \zeta^2}\left(\frac{u}{\sqrt{h}}\right) - \sqrt{2\psi}\left(\frac{\epsilon^2}{2}\frac{dh}{d\zeta}\frac{\partial Q}{\partial \zeta} + h^2\frac{\partial Q}{\partial \psi}\right)\right], \tag{44}$$

$$-\epsilon^2\Omega^2\xi_\varphi = \frac{h\sqrt{h}}{\rho}\left[\frac{\epsilon^2}{\mu_0}\frac{\partial^2(\xi_\varphi\sqrt{h})}{\partial \zeta^2} - \frac{ih}{\sqrt{2\psi}}Q\right], \tag{45}$$

$$Q = \frac{-1}{\mu_0\sqrt{2h\psi}}\left(\epsilon^2\frac{\psi}{h^2}\frac{dh}{d\zeta}\frac{\partial u}{\partial \zeta} + 2\psi\frac{\partial u}{\partial \psi} + u + ih\xi_\varphi\right). \tag{46}$$

The system of equations (44)–(46) contains the small parameter ϵ^2. This inspires us to look for a solution to this system in the form of expansions in power series with respect to ϵ^2. We assume that u and ξ_φ are the quantities of the order of unity. Then, it follows from equation (45) that Q is of the order of ϵ^2, and we write the expansions for u, ξ_φ, and Q as

$$u = u_1 + \epsilon^2 u_2 + \ldots,$$
$$\xi_\varphi = \xi_{\varphi 1} + \epsilon^2\xi_{\varphi 2} + \ldots,$$
$$Q = \epsilon^2 Q_1 + \epsilon^4 Q_2 + \ldots. \tag{47}$$

Substituting equation (47) in equations (44)–(46) and collecting the largest terms in each of these equations, we obtain

$$\frac{h}{\mu_0}\frac{\partial^2}{\partial \zeta^2}\left(\frac{u_1}{\sqrt{h}}\right) - h^2\sqrt{2\psi}\frac{\partial Q_1}{\partial \psi} + \frac{\rho\Omega^2}{h\sqrt{h}}u_1 = 0, \tag{48}$$

$$\frac{1}{\mu_0}\frac{\partial^2(\xi_{\varphi 1}\sqrt{h})}{\partial \zeta^2} - \frac{ih}{\sqrt{2\psi}}Q_1 + \frac{\rho\Omega^2}{h\sqrt{h}}\xi_{\varphi 1} = 0, \tag{49}$$

$$2\psi\frac{\partial u_1}{\partial \psi} + u_1 + ih\xi_{\varphi 1} = 0. \tag{50}$$

Eliminating $\xi_{\varphi 1}$ from equations (49) and (50) yields

$$Q_1 = \frac{2\psi}{h\mu_0}\left(\frac{\partial^2}{\partial \zeta^2} + \frac{\mu_0\rho\Omega^2}{h^2}\right)\frac{\partial U}{\partial \psi}, \tag{51}$$

where

$$U = \sqrt{\frac{2\psi}{h}}u_1. \tag{52}$$

Substituting this expression in equation (48), we arrive at

$$\left(\frac{\partial^2}{\partial \zeta^2} + \frac{\mu_0\rho\Omega^2}{h^2}\right)\left[4\psi\frac{\partial}{\partial \psi}\left(\psi\frac{\partial U}{\partial \psi}\right) - U\right] = 0. \tag{53}$$

It follows from the frozen-in conditions that

$$U = 0 \quad \text{at } \zeta = \pm\epsilon L. \tag{54}$$

The Sturm-Liouville problem

$$\frac{\partial^2 f}{\partial \zeta^2} + \frac{\mu_0\rho\Omega^2}{h^2}f = 0, \quad f = 0 \quad \text{at } \zeta = \pm\epsilon L \tag{55}$$

describes individual oscillations of magnetic field lines with the Alfvén frequency. In what follows we assume that the frequencies of the tube kink oscillations are not close to any of the Alfvén frequencies. Then, it follows from equation (53) that

$$4\psi\frac{\partial}{\partial \psi}\left(\psi\frac{\partial U}{\partial \psi}\right) - U = 0. \tag{56}$$

It is straightforward to obtain that the general solution of equation (56) is

$$U = U_1(\zeta)\psi^{1/2} + U_2(\zeta)\psi^{-1/2}, \tag{57}$$

where $U_1(\zeta)$ and $U_2(\zeta)$ are arbitrary functions satisfying $U_1(\pm\epsilon L) = U_2(\pm\epsilon L) = 0$.

The equation of the tube boundary in the flux variables is $\psi = \psi_0$, so that the interior and exterior of the tube are determined by $\psi < \psi_0$ and $\psi > \psi_0$, respectively. Since the solution inside the tube has to be regular at $\psi = 0$, it is given by

$$U = U_1(\zeta)\psi^{1/2}. \tag{58}$$

In the case of a tube with a constant cross section, the plasma motion caused by the kink oscillation outside the tube practically decays at a distance of a few tube radii. We look for oscillations of a tube with variable cross section having the same property. Then, the solution in the region $\psi > \psi_0$ is

$$U = U_2(\zeta)\psi^{-1/2}. \tag{59}$$

Note that a weaker condition that perturbations decay as $r \to \infty$ is not sufficient to obtain equation (59). The reason for this is that equation (57) is only valid in the tube vicinity, i.e., for $r \ll L$, and cannot be used for $r \to \infty$.

To derive the equation describing the tube oscillations we have to use the boundary conditions at the tube boundary. The first of these conditions is the kinematic boundary condition $\xi_{\perp -} = \xi_{\perp +}$, where $\xi_{\perp\pm} = \lim_{\psi\to\psi_0\pm 0}\xi_\perp$. In the lowest order approximation with respect to ϵ^2, it reduces to

$$U_- = U_+. \tag{60}$$

It follows from this condition and equations (58) and (59) that

$$U_2(\zeta) = \psi_0 U_1(\zeta). \tag{61}$$

The second boundary condition is the dynamic boundary condition $P_- = P_+$. In the lowest order approximation, it reduces to

$$Q_{1-} = Q_{1+}. \tag{62}$$

Using equations (51), (58), (59), and (61), we obtain from equation (62)

$$\frac{d^2U_1}{d\zeta^2} + \frac{\Omega^2}{C_k^2}U_1 = 0, \tag{63}$$

where

$$C_k^2 = \frac{2B^2(z)}{\mu_0[\rho_i(z) + \rho_e(z)]}. \tag{64}$$

To obtain equation (64) we have used the approximate relation from equation (17).

It follows from equations (18), (37), (52), and (58) that

$$U_1 = \text{const}\frac{\xi_\perp}{R(z)} + O(\epsilon^2). \tag{65}$$

Hence, in the lowest order approximation with respect to ϵ^2, we can substitute

$$\eta = \frac{\xi_\perp}{R(z)} \tag{66}$$

for U_1 in equation (63). Then, returning to the original variable z, we conclude that the eigenfrequencies and eigenmodes of the tube kink oscillations are determined by the Sturm-Liouville problem

$$\frac{d^2\eta}{dz^2} + \frac{\omega^2}{C_k^2}\eta = 0, \quad \eta = 0 \quad \text{at } z = \pm L, \tag{67}$$

where $C_k(z)$ is given by equation (64). This result is a generalization of the result obtained by Dymova & Ruderman (2005) for a tube with a constant cross section.

As we have already mentioned in § 1, recently the transverse oscillations of a longitudinally stratified tube with a variable cross section was studied by Verth & Erdélyi (2008). These authors derived the equation determining the eigenmodes and eigenfunctions of kink tube oscillations assuming that the tube expansion is small. To assess the accuracy of the approximate equation derived by Verth & Erdélyi (2008), we compare the frequencies calculated using equation (67) valid for an arbitrary expansion factor and the equation of Verth & Erdélyi valid only for expansion factors close to unity. When doing so we assume that there is no density stratification. For the magnetic field we use the model described in § 2 as an example. We take $l = L/3$. Then, in accordance with equation (13), the restriction for the expansion factor is $\lambda < \lambda_m \approx 1.67$. The results of our calculations are presented in Figure 2. The dependencies of the fundamental frequency and the frequency of the first overtone are shown. We see that both frequencies decrease when λ increases. It is not surprising at all, because the total magnetic tension at fixed z, which is proportional to $B^2(z)R^2(z) \sim R^{-2}(z)$, decreases [recall that $B(z)R^2(z) \approx$ const]. Note the very good agreement between the results obtained with the use of equation (67) valid for an arbitrary expansion factor and those obtained with the use of the equation valid only for expansion factors close to unity. Hence, although Verth & Erdélyi (2008) derived their equation under the assumption $\lambda - 1 \ll 1$, it seems that it remains valid for $\lambda - 1 \sim 1$. Finally, we note a very unusual situation: the equation derived in this paper for an arbitrary expansion factor is simpler than the equation derived by Verth & Erdélyi (2008) for expansion factors close to unity.

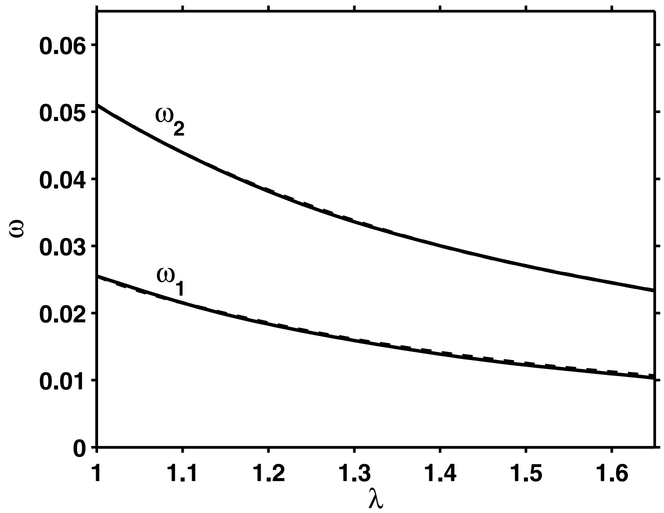

FIG. 2.—Dependencies of frequencies of the fundamental kink mode, ω_1, and the first overtone, ω_2, on the expansion factor λ. The solid curves were obtained using eq. (67) of this paper, while the dashed curves were obtained using the approximate equation by Verth & Erdélyi (2008).

We have to emphasize that the comparison of our results with the results obtained by Verth & Erdélyi (2008) as well as the calculation of dependences of ω_1 and ω_2 on λ has been carried out for only one particular equilibrium state. Of course, the numerical values will change if we consider another equilibrium state, in particular, if we choose another value of l. However, we anticipate that qualitatively the results will be the same.

5. IMPLICATION FOR CORONAL SEISMOLOGY

Verwichte et al. (2004) reported two cases of observation of transverse coronal loop oscillations where both the fundamental mode and first overtone were detected. The frequency of the first overtone was smaller than the double frequency of the fundamental mode. Andries et al. (2005a) suggested that this effect was caused by the density variation along the loop. Assuming that the plasma in the coronal loop is isothermal and that the loop has the shape of a semicircle in the vertical plane, they used the ratio of frequencies of the fundamental harmonic and first overtone to estimate the density scale height.

Recently, Van Doorsselaere et al. (2007) reported a new case of simultaneous observation of the fundamental mode and first overtone in the transverse coronal loop oscillation. They also revisited the observations reported by Verwichte et al. (2004) using an improved technique that reduces the uncertainties in the determination of the oscillation periods.

Dymova & Ruderman (2006b) studied the effect of the loop shape on the determination of the density scale height using the ratio of frequencies of the fundamental harmonic and first overtone. They considered a loop with the shape of an arc of a circle and found that the dependence of the calculated density scale height on the loop shape is fairly strong. McEwan et al. (2008) studied the dependence of the ratio of the fundamental frequency and the frequency of the first overtone on the atmospheric scale height in an exponentially stratified loop.

In this paper we study the effect of cross-sectional area variation on the determination of density scale height. We assume that the loop has the shape of a half-circle of radius $2L/\pi$. The plasma is assumed to be isothermal with the same temperature inside and outside the loop, so that $\rho_i = \hat{\rho}_i e^{-h/H}$ and $\rho_e = \hat{\rho}_e e^{-h/H}$, where h is the height in the atmosphere and H is the density scale height. Since

$$h = \frac{2L}{\pi}\cos\frac{\pi z}{2L},$$

we obtain

$$\rho_i = \hat{\rho}_i \exp\left(-\frac{2L}{\pi H}\cos\frac{\pi z}{2L}\right),$$
$$\rho_e = \hat{\rho}_e \exp\left(-\frac{2L}{\pi H}\cos\frac{\pi z}{2L}\right). \quad (68)$$

We once again consider a particular magnetic field configuration described in § 2. Then, using equation (14) determining $R(z)$, the relation $B(z)R^2(z) = \text{const}$, and equation (68), we obtain

$$C_k = C_{kf}\exp\left(-\frac{L}{\pi H}\cos\frac{\pi z}{2L}\right) \times \frac{\cosh(L/l) - \lambda^2 + (\lambda^2 - 1)\cosh(z/l)}{\lambda^2[\cosh(L/l) - 1]}, \quad (69)$$

where $C_{kf} = C_k(\pm L)$ is the value of $C_k(z)$ at the footpoints. In our calculations we took $l = L/3$, which reduces equation (69) to

$$C_k = \frac{C_{kf}}{\lambda^2}\exp\left(-\frac{L}{\pi H}\cos\frac{\pi z}{2L}\right) \times \left\{1 + 0.11(\lambda^2 - 1)[\cosh(3z/L) - 1]\right\}. \quad (70)$$

After that we used the same procedure as in Dymova & Ruderman (2006b). We fixed λ and solved equation (67) numerically with C_k given by equation (70). As a result, we found the dependence of the ratio of the first overtone to the fundamental harmonic, ω_2/ω_1, as a function of L/H. Since both ω_2/ω_1 and the loop height $2L/\pi$ are known from the observations reported by Verwichte et al. (2004) and Van Doorsselaere et al. (2007), we can eventually determine the scale height H. Recall that, in accordance with the improved analysis by Van Doorsselaere et al. (2007), $\omega_2/\omega_1 = 1.82$ and $2L = 218$ Mm in the first case reported by Verwichte et al. (2004), while $\omega_2/\omega_1 = 1.58$ and $2L = 228$ Mm in the second case. In the case reported by Van Doorsselaere et al. (2007; case three) these quantities were given by $\omega_2/\omega_1 = 1.795$ and $2L = 400$ Mm. For $\lambda = 1$ these values give $H = 68$, 30, and 109 Mm for the first, second, and third cases, respectively. Then we calculated H for λ varying from 1 to 1.65. As a result, we found the dependencies of H on the expansion factor λ for these three cases. The results of our calculations are presented in Figure 3. We see that the scale height is a decreasing function of λ.

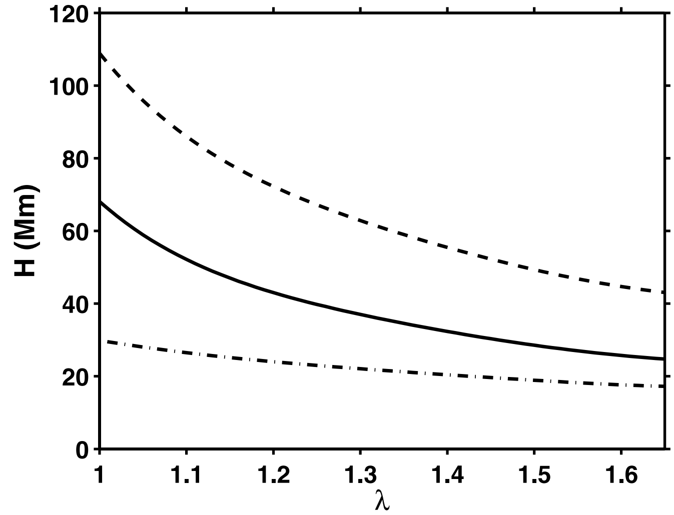

FIG. 3.—Solid and dash-dotted curves show the dependencies of the scale height H on the expansion factor λ for the two cases reported by Verwichte et al. (2004). The dashed curve shows the dependence of H on λ for the case reported by Van Doorsselaere et al. (2007).

Van Doorsselaere et al. (2007) discussed why the obtained scale height of the loop considered in their paper was more than two times larger than the hydrostatically expected value 50 Mm. We can see that one possible explanation is that they did not take the loop expansion into account. We obtain $H \approx 50$ Mm for this loop if we take $\lambda \approx 1.5$, which is definitely not an unrealistic value. On the other hand, we note that the estimate of the scale height obtained by Van Doorsselaere et al. (2007) is consistent with the independent estimate given by Aschwanden et al. (2000). So it is quite possible that, in this particular case, the expansion factor was very close to unity.

6. SUMMARY AND CONCLUSIONS

In this paper we have studied the fast kink oscillations of longitudinally stratified magnetic tubes with circular variable cross-sectional area. The tube axis was assumed to be straight, and the tube ends to be frozen in the dense photospheric plasma. We considered a thin tube with the ratio of the tube radius to length of the order of $\epsilon \ll 1$. We restricted our study to the eigenmodes with all quantities proportional to $e^{-i\omega t}$. Then we used the method of asymptotic expansions to derive the second-order ordinary differential equation for the displacement of the tube axis. This equation is a generalization of the corresponding equation derived by Dymova & Ruderman (2005) for longitudinally stratified magnetic tubes with a constant radius. The boundary conditions at the tube ends and this equation together constitute the Sturm-Liouville problem that determines the eigenfrequencies and eigenfunctions of the tube kink oscillations.

We discussed the implications of our results on coronal seismology. We concentrated on the method of estimation of the coronal scale height H using the ratio of periods of the fundamental kink mode and the first overtone that was suggested by

Andries et al. (2005a). We showed that this method is very sensitive to the tube expansion factor λ, which is the ratio of the tube radii at the apex and footpoints. Our main result is that the estimated coronal scale height is a monotonically decreasing function of λ. A particularly striking example is related to the estimate of the coronal scale height presented by Van Doorsselaere et al. (2007). These authors considered one of the observations of coronal loop kink oscillations and, using the observational data, found $H \approx 109$ Mm. To obtain this estimate they used the model of a coronal loop with a constant radius. We showed that $H \approx 50$ Mm if we assume that the loop expands and take $\lambda \approx 1.5$.

This work was inspired by discussions at a workshop in Bern organized by ISSI. The authors acknowledge the financial support from STFC and EPSRC. R. E. acknowledges M. Kéray for patient encouragement and is also grateful to NSF, Hungary (OTKA, K67746).

REFERENCES

Abramowitz, M., & Stegun, I. 1964, Handbook of Mathematical Functions (Washington, DC: Natl. Bur. Stand.)
Andries, J., Arregui, I., & Goossens, M. 2005a, ApJ, 624, L57
Andries, J., Goossens, M., Hollweg, J. V., Arregui, I., & Van Doorsselaere, T. 2005b, A&A, 430, 1109
Aschwanden, M. J., Fletcher, L., Schrijver, C. J., & Alexander, D. 1999, ApJ, 520, 880
Aschwanden, M. J., Nightingale, R. W., & Alexander, D. 2000, ApJ, 541, 1059
Banerjee, D., Erdelyi, R., Oliver, R., & O'Shea, E. 2007, Sol. Phys., 246, 3
Dymova, M., & Ruderman, M. S. 2005, Sol. Phys., 229, 79
———. 2006a, A&A, 457, 1059
———. 2006b, A&A, 459, 241
Goossens, M., Andries, J., & Arregui, I. 2006, Philos. Trans. R. Soc. London A, 364, 433
McEwan, M. P., Diaz, A. J., & Roberts, B. 2008, A&A, 481, 819
Nakariakov, V. M., & Ofman, L. 2001, A&A, 372, L53
Nakariakov, V. M., Ofman, L., DeLuca, E. E., Roberts, B., & Davila, J. M. 1999, Science, 285, 862
Van Doorsselaere, T., Nakariakov, V. M., & Verwichte, E. 2007, A&A, 473, 959
Verth, G., & Erdélyi, R. 2008, A&A, 486, 1015
Verwichte, E., Nakariakov, V. M., Ofman, L., & DeLuca, E. E. 2004, Sol. Phys., 223, 77